Chapter **1**

Introduction to Suspension Rheology

Nhan PHAN-THIEN
University

1.1. Introduction

The term "suspension" is used to describe a class of fluids made up of particulate particles (rigid particles, liquid droplets and gas bubbles) suspended in a liquid, which may be Newtonian or non-Newtonian. When the suspending liquid (solvent) is Newtonian, we call it a Newtonian suspension, and if this is not the case, it is non-Newtonian suspension. Examples of suspensions include both natural and man-made materials – for instance, ink as a suspension of pigments of dyes of typically $5 - 10\ \mu m$ in a Newtonian fluid, whole blood as a suspension of mainly deformable red blood cells (of typically $8 - 12\ \mu m$ in size) in a mildly non-Newtonian fluid referred to as plasma, sediment as a suspension of rigid particles of poly-dispersed shapes and sizes ($0.1\ \mu m$ to centimeter in sizes) in water. At some scale levels, the effective fluid may be regarded as a continuum – for this to make physical sense, there must be two widely separated length scales in the problem: a is a typical dimension of a particle and L is a typical dimension of the flow apparatus, and $a \ll L$, otherwise we just simply have a collection of individual particles suspended in a liquid. In addition, every relevant representative volume must contain a sufficient number of particles so that an effective fluid property could be well defined – this is a fundamental assumption in all theoretical treatments seeking to replace the composity fluid by an effective continuum. How large a representative volume is in practice a subjective judgment, and it represents the resolution length scale in the problem. Some well-reviewed papers containing a lot of

useful information on suspensions are Gadala-Maria and Acrivos (1980), Metzner (1985) and Zarraga *et al*. (2000).

When the suspended particles are small enough, from nm to μm in size, they are subject to random bombardments of the solvent molecules, and their modeling ignoring molecular motion tends to incorporate the so-called Brownian forces, a stochastic mean of quantifying these random bombardments. The relative importance of the Brownian forces may be characterized by a PÃ©clet number, representing the ratio of viscous hydrodynamic and random Brownian forces:

$$Pe = \frac{\eta_s \dot{\gamma} \alpha^3}{k_B T}, \qquad [1.1]$$

where η_s is the solvent viscosity, $\dot{\gamma}$ is the typical shear rate and $k_B T$ is the Boltzmann temperature. When this number is low, Brownian forces dominate leading to a relatively more randomized particle orientation with a larger dissipation than when the Pe number is large, with more particles aligned with the flow. Dissipation directly links to effective viscosity and, therefore, we expect a shear-thinning property with the inclusion of Brownian motion. It is generally agreed Mewis and Wagner (2012) that particles of $10\ \mu m$ in size or larger are not significantly influenced by Brownian motion. These particles are called *non-colloidal* particles, as opposed to smaller *colloidal* particles, those smaller than about $10\ \mu m$, where the Brownian motion must be a part of their description. The Pe number corresponding to $a = 10\ \mu m$, $\eta_s = 1$ Pa.s, $\dot{\gamma} = 1\ \text{s}^{-1}$, and $T = 293$ K is of $O\left(10^5\right)$, and this may be taken as a delineating range between colloidal and non-colloidal particles. Suspension of colloidal particles is referred to as colloidal suspension, and that of non-colloidal particles is referred to as non-colloidal suspension. Excellent books and reviews on colloidal suspensions exist (e.g. Mewis and Wagner (2012) and Morris (2009), to which we refer the readers).

An excellent theoretical framework has been built up in understanding non-colloidal Newtonian suspensions in the dilute limit, and this is the focus of this chapter. We concentrate on a representative volume $V = V_p \cup V_f$, where V_p is the volume occupied by the particles and V_f is the volume occupied by the Newtonian solvent. With $a \ll L$, the relevant Reynolds number is small and the micromechanics of particles in V follow the Stokes equations:

$$\nabla \cdot \mathbf{u} = 0, \quad -\nabla p + \eta_s \nabla^2 \mathbf{u} = \mathbf{0}, \ \text{ in } V \backslash V_p, \qquad [1.2]$$

subjected to some relevant boundary conditions on the bounding surface of $V \backslash V_p$. Since the governing equations are linear and instantaneous, the micromechanics are also linear and instantaneous on the driving boundary data: when the flow stops, the micromechanics cease instantaneously. As a result, the stress contributed by particles

would be linear in the velocity gradient (the driving force), and would be zeroed instantly once the flow is stopped. The fluid would have no memory at cessation of flow – any relaxation would have to come from the viscoelastic solvent, which is not modeled by [1.2]. The microstructure, as represented by the volume fraction and the configuration of particles, evolves with the flow and, therefore, endows a memory to the fluid at start-up. When the microstructure has reached a steady state, the particle-contributed stress would also reach a steady state. At this point, the flow may be stopped and the micromechanics cease instantly, freezing the particles configuration in place. The flow may be started again in the same direction, and the particles configuration would continue from its steady state without any further evolving, and the particle-contributed stress would assume its previous value just before the flow was stopped. The flow has no relaxation upon starting, and the period of rest does not matter, because there is no microinertia. However, if the flow is restarted in the opposite direction, then the particle microstructure, not being in the steady-state configuration with respect to this flow, readjusts itself in the same manner as if it restarting afresh from its initial state, and therefore endows the fluid with a memory as before. Thus, by simply considering the nature of the micromechanics, explanation to some experimental observations of Gadala-Maria and Acrivos Gadala-Maria and Acrivos (1980) can be provided.

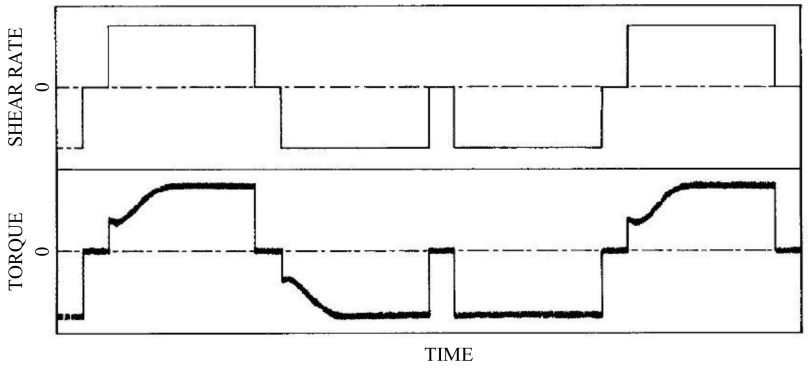

Figure 1.1. *Start and stop shear flow experiment; the torque would be proportional to the shear stress, after Gadala-Maria and Acrivos Gadala-Maria and Acrivos (1980)*

1.2. General bulk suspension properties

1.2.1. *Bulk stress and stresslet*

We now consider a representative volume $V = V_p \cup V_f$, which is large enough to contain many particles but small enough so that macroscopic variables hardly change on the scale $V^{1/3}$, i.e. $a \ll V^{1/3} \ll L$. The existence of such representative volume is taken as an assumption in most works dealing with properties of an effective continuum (i.e. *homogenization*). The effective stress tensor seen from a macroscopic level is simply the volume-averaged stress Landau and Lifshitz (1959):

$$\langle \sigma \rangle = \frac{1}{V} \int_V \sigma \, dV = \frac{1}{V} \int_{V_f} \sigma dV + \frac{1}{V} \int_{V_p} \sigma dV, \qquad [1.3]$$

where the angle brackets denote a volume-averaged quantity. With a Newtonian solvent, the stress is a hydrostatic pressure plus an extra stress proportional to the strain rate tensor $D_{ij} = \left(\partial u_i/\partial x_j + \partial u_j/\partial x_i\right)/2$ ($\mathbf{u}$ is the imposed velocity vector):

$$\sigma(\mathbf{x}) = -P\mathbf{I} + 2\eta_s \mathbf{D} \equiv \sigma^{(f)}, \quad \mathbf{x} \in V_f.$$

Thus:

$$\frac{1}{V} \int_{V_f} \sigma dV = -\langle P \rangle \mathbf{I} + 2\eta_s \langle \mathbf{D} \rangle - \frac{1}{V} \int_{V_p} \sigma^{(f)} dV.$$

Furthermore, in the absence of microinertia and the body force, the micromechanics must satisfy the balance of momentum (using Cartesian tensor notation) $\partial \sigma_{ij}/\partial x_j = 0$, which implies:

$$\frac{\partial}{\partial x_k} \left(x_i \sigma_{kj}\right) = \sigma_{ij},$$

and we find that:

$$\frac{1}{V} \int_{V_p} \sigma_{ij} \, dV = \frac{1}{V} \int_{V_p} \frac{\partial}{\partial x_k} \left(x_i \sigma_{kj}\right) \, dV = \frac{1}{V} \int_{S_p} x_i t_j \, dS, \qquad [1.4]$$

where $t_j = \sigma_{kj} n_k$ is the traction vector and the divergence theorem has been used to convert the volume integral into a surface integral over the bounding surface S_p

of all the particles. In addition, with the Newtonian solvent assumption and using the divergence theorem:

$$\frac{1}{V}\int_{V_p}\sigma_{ij}^{(f)}\,dV = \frac{1}{V}\int_{V_p}\left[-P\delta_{ij}+\eta_s\left(\frac{\partial u_i}{\partial x_j}+\frac{\partial u_j}{\partial x_i}\right)\right]\,dV$$
$$= -P_1\delta_{ij}+\frac{1}{V}\int_{S_p}\left[\eta_s\left(u_i n_j+u_j n_i\right)\right]\,dS$$

where P_1 is the scalar pressure. The average stress is thus given by:

$$\langle\sigma_{ij}\rangle = -P'\delta_{ij}+\underbrace{2\eta_s\langle D_{ij}\rangle}_{\text{solvent}}+\underbrace{\frac{1}{V}\int_{S_p}\left\{x_i t_j-\eta_s\left(u_i n_j+u_j n_i\right)\right\}\,dS}_{\text{particles}}, \quad [1.5]$$

consisting of a solvent contribution and a particle contribution; P' is just a scalar pressure (the prime will be dropped from hereon). The particle contribution can be decomposed into a symmetric part and an antisymmetric part. The symmetric part is, in fact, the sum of the *stresslets* $\mathcal{S}_{ij}^{(p)}$ defined by Batchelor (1970):

$$\mathcal{S}_{ij} = \frac{1}{2}\int_{S_p}\left\{x_i t_j+x_j t_i-2\eta_s\left(u_i n_j+u_j n_i\right)\right\}\,dS = \sum_p \mathcal{S}_{ij}^{(p)}, \quad [1.6]$$

and the antisymmetric part leads to the rotlet Batchelor (1970):

$$\mathcal{R}_{ij} = \frac{1}{2}\int_{S_p}\left(x_i t_j-x_j t_i\right)\,dS = \frac{1}{2}\sum_p \epsilon_{ijk}T_k^{(p)}, \quad [1.7]$$

where $T_k^{(p)}$ is the torque exerted on the particle p, ε_{ijk} is the alternating tensor and the summation is over all particles in the volume V. The particle-contributed stress is, therefore, given by:

$$\sigma_{ij}^{(p)} = \frac{1}{V}\sum_p\left(\mathcal{S}_{ij}^{(p)}+\frac{1}{2}\epsilon_{ijk}T_k^{(p)}\right). \quad [1.8]$$

A more general approach for calculating stresslet for a general particle based on singularity multipole expansion and/or FaxÃ©n theorem is detailed in Kim (1991), with a parallel development in elasticity in Phan-Thien and Kim (1994).

1.2.2. *Bulk dissipation*

Sometimes, it is desirable to compute the total rate of energy dissipation. By considering a volume V large enough to contain all the particles, the total rate of energy dissipation in V is thus:

$$\Phi = \int_V \sigma_{ij} D_{ij} \, dV = \int_V \frac{\partial}{\partial x_j} \left(\sigma_{ij} u_i \right) \, dV = \sum_p \int_{S_p} \sigma_{ij} u_i n_j \, dS. \qquad [1.9]$$

The second equality comes from the balance of momentum, and the third equality comes from an application of the divergence theorem, assuming that the condition at infinity is quiescent (the bounding surface of V consists of particles' surfaces and surface at infinity). For a system of rigid particles, the boundary condition on the surface of a particle p is that:

$$\mathbf{u} = \mathbf{U}^{(p)} + \mathbf{\Omega}^{(p)} \times \mathbf{x}, \qquad [1.10]$$

where $\mathbf{U}^{(p)}$ and $\mathbf{\Omega}^{(p)}$ are the translational and rotation velocities of the particle, which can be taken outside the integral in [1.9], and the remaining integrals can be identified with the force $\mathbf{F}^{(p)}$ and the torque $\mathbf{T}^{(p)}$ imparted by the particle p to the fluid. Thus, the total rate of energy dissipation is:

$$\Phi = \sum_p \left(\mathbf{U}^{(p)} \cdot \mathbf{F}^{(p)} + \mathbf{\Omega}^{(p)} \cdot \mathbf{T}^{(p)} \right). \qquad [1.11]$$

Note also that for a system of rigid particles, the integral:

$$\int_{S_p} \left(\mathbf{un} + \mathbf{nu} \right) dS = \mathbf{0},$$

since:

$$\int_{S_p} \mathbf{U}^{(p)} \mathbf{n} dS = \mathbf{0}, \quad \int_{S_p} \left(\mathbf{\Omega}^{(p)} \times \mathbf{xn} + \mathbf{n} \mathbf{\Omega}^{(p)} \times \mathbf{x} \right) dS = \mathbf{0},$$

by applications of the divergence theorem.

1.3. Dilute suspension of rigid spheres

1.3.1. *Stresslet*

We now consider a dilute suspension of force- and torque-free monodispersed spheres, of radius a each, in an ambient uniform flow $\mathbf{U}$ superimposed by shear flow of velocity gradient $\mathbf{L} = \mathbf{D} + \mathbf{W}$, where $\mathbf{D}$ is the strain rate tensor and $\mathbf{W}$, the vorticity tensor. Dilute concentration means the volume fraction:

$$\phi = \nu \frac{4\pi a^3}{3} \ll 1, \qquad [1.12]$$

where ν is the number density of the spheres. In this case, in a representative volume V, we expect to find only one sphere in isolation. Thus, the micromechanic problem consists of a single sphere in an effectively unbounded fluid – unbounded here means far away from the particle concerned, but still not far enough to run into another sphere. The relevant boundary conditions for this micromechanic problem are:

$$\mathbf{u}(\mathbf{x}) = \mathbf{U} + (\mathbf{D} + \mathbf{W}) \cdot \mathbf{x}, \quad \text{far from the particle, } |\mathbf{x}| \to \infty, \qquad [1.13]$$

and

$$\mathbf{u}(\mathbf{x}) = \mathbf{V} + \mathbf{w} \cdot \mathbf{x}, \quad \text{on the particle's surface, } |\mathbf{x}| = a. \qquad [1.14]$$

Here, $(\mathbf{V}, \mathbf{w})$ constitute a rigid body motion of the particle, with $\mathbf{V}$ its translational motion and $\mathbf{w}$ a skew-symmetric tensor such that $w_{ij} = -\epsilon_{ijk}\Omega_k$, where $\mathbf{\Omega}$ is the angular velocity of the particle. The solution to this unbounded flow problem can be generated from Lamb's solution Happel and Brenner (1973), or it can be synthesized from Stokes' singular solution Phan-Thien and Kim (1994):

$$\begin{aligned}\mathbf{u} = \mathbf{U} + \mathbf{L} \cdot \mathbf{x} + \frac{a^3}{x^3}(\mathbf{w} - \mathbf{W}) \cdot \mathbf{x} + \left(\frac{3a}{4x} + \frac{a^3}{4x^3}\right)(\mathbf{V} - \mathbf{U}) - \frac{a^5}{x^5}\mathbf{D} \cdot \mathbf{x} \\ + \frac{3a}{x^3}\left(1 - \frac{a^2}{x^2}\right)(\mathbf{V} - \mathbf{U}) \cdot \mathbf{xx} - \frac{5a^3}{2x^5}\left(1 - \frac{a^2}{x^2}\right)\mathbf{D} : \mathbf{xxx}, \qquad [1.15]\end{aligned}$$

and

$$P = \frac{3}{2}\eta_s \frac{a}{x^3}(\mathbf{V} - \mathbf{U}) \cdot \mathbf{x} - 5\eta_s \frac{a^3}{x^5}\mathbf{D} : \mathbf{xx}. \qquad [1.16]$$

From this, the strain rate tensor and the stress can be calculated leading to the traction on the surface of the sphere:

$$\mathbf{t} = \sigma \cdot \mathbf{n}|_{x=a} = -\frac{3\eta_s}{2a}(\mathbf{V} - \mathbf{U}) - \frac{3\eta_s}{a}(\mathbf{w} - \mathbf{W}) \cdot \mathbf{x} + 5\frac{\eta_s}{a}\mathbf{D} \cdot \mathbf{x}. \qquad [1.17]$$

The force and the torque on the particle can be evaluated:

$$\mathbf{F} = \int_S \sigma \cdot \mathbf{n}\, dS = -6\pi\eta_s a(\mathbf{V} - \mathbf{U}) \qquad [1.18]$$

and

$$\mathbf{T} = \int_S \mathbf{x} \times \sigma \cdot \mathbf{n} dS = -8\pi\eta_s a^3(\mathbf{\Omega} - \omega), \qquad [1.19]$$

where $\omega_i = \frac{1}{2}\epsilon_{ijk}W_{jk}$ is the local vorticity vector. Thus, if the particle is force-free and torque-free, then it translates with $\mathbf{U}$ and spin with an angular velocity of ω.

Returning now to the particle-contributed stress, [1.8],

$$\left\langle \sigma_{ij}^{(p)} \right\rangle = \frac{1}{V}\sum_p \mathcal{S}_{ij} = \nu\mathcal{S}_{ij},$$

where the stresslet is given in [1.6]. From [1.17], and noting that

$$\int_S \mathbf{x}\, dS = \mathbf{0}, \quad \int_S \mathbf{xx}\, dS = \frac{4\pi a^4}{3}\mathbf{1},$$

we find

$$\mathcal{S}_{ij} = \frac{1}{2}\int_S (x_i t_j + x_j t_i)\ dS = 5\frac{\eta_s}{a}\int_S D_{ik}x_k x_j\, dS = 5\eta_s\left(\frac{4\pi a^3}{3}\right)D_{ij}.$$

Recall that the volume fraction of particles is $\phi = 4\pi a^3\nu/3$; the total effective stress, consisted of the solvent stress and the particle-contributed stress, will now become:

$$\langle\sigma\rangle = -P\mathbf{1} + 2\eta_s\left(1 + \frac{5}{2}\phi\right)\mathbf{D}, \qquad [1.20]$$

and consequently the dilute suspension is Newtonian, with a reduced viscosity of:

$$\mu_r = \frac{\eta}{\eta_s} = 1 + \frac{5}{2}\phi. \qquad [1.21]$$

This is the celebrated Einstein result Einstein (1956), who arrived at the conclusion from the equality of the dissipation at the microscale and the macroscale as described by an effective Newtonian viscosity. It is generally agreed that [1.21] is quite accurate at a volume fraction $\phi < 0.02$. Current research aims to understand moderate to concentrated suspensions, for both Newtonian Foss and Brady (2000), Zarraga *et al*. (2000), Pan *et al*. (2010), Dai *et al*. (2013), Lin *et al*. (2014) and non-Newtonian suspensions Lyon *et al*. (2001), Zarraga *et al*. (2001), Mall-Gleissle *et al*. (2002), Tanner *et al*. (2010)); not surprisingly, due to the complex nature of the fluids, most of these studies are numerical modeling in nature.

1.3.2. *An exact poly-dispersed model*

Although the limitation on [1.21] is quite severe, it may be used to arrive at an exact theoretical construction for a poly-dispersed suspension at an arbitrary volume fraction, which could provide some guidance into an experimental correlation. The process starts by adding a small infinitesimal volume $\Delta\phi$ of the particulate rigid phase of size a. The effective medium is Newtonian, and its viscosity is given by:

$$\eta' = \eta_s \left(1 + \frac{5}{2}\Delta\phi\right). \qquad [1.22]$$

To this effective Newtonian medium, another infinitesimal volume fraction of particulate rigid phase, of considerably larger size than that of the previous step, is added. This process continues until a finite volume fraction $0 < \phi < 1$ is built up. At an intermediate step, denote the viscosity at volume fraction ϕ by η. To a normalized unit volume of this, we add a $\Delta\phi$ volume of a particulate phase, of volume fraction $\Delta\phi/(1+\Delta\phi)$. This results in an effective Newtonian fluid of viscosity:

$$\eta + d\eta = \eta\left(1 + \frac{5}{2}\frac{\Delta\phi}{1+\Delta\phi}\right).$$

Since in a volume $(1+\Delta\phi)$ of the suspension, there has been a volume ϕ of the particulate phase, now augmented by $\Delta\phi$, the actual volume fraction has been increased by:

$$d\phi = \frac{\phi + \Delta\phi}{1+\Delta\phi} - \phi = \frac{\Delta\phi}{1+\Delta\phi}(1-\phi),$$

and, therefore, we can build up the following differential model for the viscosity:

$$\frac{d\eta}{\eta} = \frac{5d\phi}{2\left(1-\phi\right)}$$

which can be integrated, subjected to $\eta\left(\phi=0\right)=\eta_s$ to yield:

$$\frac{\eta}{\eta_s} = \frac{1}{\left(1-\phi\right)^{5/2}}. \qquad [1.23]$$

This relation was proposed and investigated by Roscoe Roscoe (1952). He noted that the relation works well for poly-dispersed suspensions of spheres at low volume fraction; however, as the relation allows for a maximum packing ratio of $\phi = 1$, he recommended that, at high volume fraction, ϕ should be replaced by ϕ/ϕ_m, where $\phi_m \approx 0.74$ for a better agreement with experimental data.

This construction is called a *differential scheme* in composite materials Norris (1985), A.N. Norris and Sheng (1985). There have been several results reported by Phan-Thien and Pham Phan-Thien and Pham (1997) for viscosity and elasticity models of multiphase materials; the particulate phases may be rigid, droplets and bubbles, or a combination of them. Recently, Tanner *et al*. Tanner *et al*. (2010) reported a differential scheme for a weakly viscoelastic solvent.

1.4. Dilute suspension of spherical droplets

Small droplets (made up of an incompressible Newtonian fluid) do not suffer significantly in their deformation and can be considered spherical as they are transported in the flow. Their analysis is complicated by the fact that the interior flow has to match with the exterior flow on their surfaces, and the extra parameter:

$$\lambda = \frac{\eta_d}{\eta_s}, \qquad [1.24]$$

the ratio of interior to exterior viscosity comes into play. Here, the solution for a droplet is available from the literature, which can be used in a similar manner to generate the stresslet. The readers are referred to Kim (1991) for an elegant treatment of FaxÃ©n theorem leading to the main result that the suspension is Newtonian, with an effective reduced viscosity of:

$$\mu_r = \frac{\eta}{\eta_s} = 1 + \frac{2+5\lambda}{2\left(1+\lambda\right)}\phi, \qquad [1.25]$$

which reduces to Einstein's relation when $\lambda \to \infty$ (for a rigid droplet suspension). For a dilute suspension of gas bubbles ($\lambda = 0$),

$$\mu_r = \frac{\eta}{\eta_s} = 1 + \phi. \qquad [1.26]$$

Relations for poly-dispersed suspensions similar to [1.23] are also available. For instance, a poly-dispersed suspension of droplets of viscosity ratio λ, constructed in the manner of a differential scheme, would have an effective viscosity implicitly given by:

$$\phi = 1 - \mu_r^{-2/5} \left(\frac{2 + 5\lambda}{2\mu_r + 5\lambda} \right)^{3/5}. \qquad [1.27]$$

1.5. Dilute suspension of rigid spheroids

1.5.1. *Jeffery's solution and stress rule*

For a dilute suspension of spheroids, a similar theory to the suspension of spheres has been worked out by Leal and Hinch Leal and Hinch (1973) using Jeffery's solution Jeffery (1922). Here, if $\mathbf{p}$ denotes a unit vector directed along the major axis of the spheroid, then Jeffery's solution states that:

$$\begin{aligned} \dot{\mathbf{p}} &= \mathbf{W} \cdot \mathbf{p} + \frac{R^2 - 1}{R^2 + 1} \left(\mathbf{D} \cdot \mathbf{p} - \mathbf{D} : \mathbf{ppp} \right), \qquad [1.28] \\ &= \mathbf{L} \cdot \mathbf{p} - \frac{2}{R^2 + 1} \mathbf{D} \cdot \mathbf{p} - \frac{R^2 - 1}{R^2 + 1} \mathbf{D} : \mathbf{ppp} \end{aligned}$$

where R is the aspect ratio of the particle (major to minor diameter ratio). The evolution of $\mathbf{p}$ is also referred to as Jeffery's orbit. Usually, the effects of Brownian motion are also included as white noise perpendicular to $\mathbf{p}$ on the right-hand side of [1.28], so as to preserve the unit length of $\mathbf{p}$. Here, $\mathbf{L} = \mathbf{D} + \mathbf{W}$ is the velocity gradient, where $\mathbf{D}$ is the strain rate and $\mathbf{W}$ is the vorticity tensor.

To complete the constitutive description of the suspension, a stress rule on how to calculate the stress from the evolving microstructure (as represented by $\mathbf{p}$) must be provided. There have been many paths to accomplish this goal. In the continuum path, we may select a relevant structure tensor (for example, $\mathbf{pp}$) and postulate that the stress is a functional of this structure tensor and a kinematic measure (for example, the strain rate tensor). From this general assumption, we can construct continuum models that satisfy various principles that we know all physical models must follow, and

restrict them to behave in the manner required by the physics of the micromechanics (for example, linear and instantaneous responses). Notable contributions from this approach are given by Hand Hand (1961) and Ericksen Ericksen (1960). We can also build up models based on a generic type of interactions, for example the spheres model of Goddard and Miller Goddard and Miller (1967), the transverse isotropic fiber model of Folgar and Tucker Folgar and Tucker (1984) and the concentrated suspension model of Phan-Thien *et al*. Phan-Thien *et al*. (1999). We will see more of this approach in this book. These models tend to mimic certain aspects of the micromechanics provided by the more exact and rigorous framework of dilute suspension of spheroids.

In the case of a dilute suspension of rigid spheroids, the stresslet is expressed in terms of some elliptic integrals Kim (1991), which can be extracted asymptotically to yield, for the particle-contributed stress Leal and Hinch (1973):

$$\sigma^{(p)} = 2\eta_s\phi\{A\mathbf{D} : \langle\mathbf{pppp}\rangle + B\left(\mathbf{D}\cdot\langle\mathbf{pp}\rangle + \langle\mathbf{pp}\rangle\cdot\mathbf{D}\right) + C\mathbf{D} + d_R F\langle\mathbf{pp}\rangle\}, \quad [1.29]$$

where the angular brackets denote the ensemble average with respect to the distribution function of $\mathbf{p}$ if stochastic noise is used to model the Brownian interaction in [1.28]; A, B, C and F are some shape factors, and d_R is the rotational diffusivity. If the particles are large enough so that Brownian motion can be ignored, then the last term, as well as the angular brackets, can be omitted in [1.29]. The asymptotic values of the shape factors have been evaluated by Leal and Hinch Leal and Hinch (1973); they are given in Table 1.1.

1.5.2. *Jeffery's orbit*

Jeffery's equation is solved by:

$$\mathbf{p} = \frac{\mathbf{Q}}{Q}, \quad [1.30]$$

where:

$$\dot{\mathbf{Q}} = \mathcal{L}\cdot\mathbf{Q}, \quad \mathcal{L} = \mathbf{L} - \frac{2}{R^2+1}\mathbf{D}, \quad [1.31]$$

as can be verified directly, $\dot{\mathbf{Q}} = \dot{\mathbf{p}}Q + \mathbf{p}\dot{Q}$. With $\mathbf{p}$ a unit vector, $\dot{\mathbf{p}}\cdot\mathbf{p} = 0$, this yields:

$$\dot{Q} = \mathbf{p}\cdot\dot{\mathbf{Q}} = Q\left(1 - \frac{2}{R^2+1}\right)\mathbf{D} : \mathbf{pp}$$
$$= Q\frac{R^2-1}{R^2+1}\mathbf{D} : \mathbf{pp}.$$

Asymptotic limit	$R \to \infty$ (rod-like)	$R = 1 + \delta,\ \delta \ll 1$ (near-sphere)	$R \to 0$ (disk-like)
A	$\dfrac{R^2}{2(\ln 2R - 1.5)}$	$\dfrac{395}{147}\delta^2$	$\dfrac{10}{3\pi R} + \dfrac{208}{9\pi^2} - 2$
B	$\dfrac{6\ln 2R - 11}{R^2}$	$\dfrac{15}{14}\delta - \dfrac{395}{588}\delta^2$	$-\dfrac{8}{3\pi R} + 1 - \dfrac{128}{9\pi^2}$
C	2	$\dfrac{5}{2}\left(1 - \dfrac{2}{7}\delta + \dfrac{1}{3}\delta^2\right)$	$\dfrac{8}{3\pi R}$
F	$\dfrac{3R^2}{\ln 2R - 1/2}$	9δ	$-\dfrac{12}{\pi R}$

Table 1.1. *Asymptotic values of the shape factors, R is the aspect ratio of the particle; $R \to \infty$ represents a rod-like particle (a slender prolate spheroid, $R \approx 1$ represents a near-sphere particle and $R \to 0$ represents a disk-like particle (flat oblate spheroid)*

When this is substituted back to $\dot{\mathbf{p}}Q = \dot{\mathbf{Q}} - \mathbf{p}\dot{Q}$, we obtain:

$$\dot{\mathbf{p}}Q = \left(\mathbf{L} - \frac{2}{R^2+1}\mathbf{D}\right)Q\mathbf{p} - Q\frac{R^2-1}{R^2+1}\mathbf{D} : \mathbf{ppp}$$

leading to equation [1.28]. The main advantage of this is that we only have to deal with a linear system [1.31], instead of the nonlinearity in [1.28]. In addition, when Brownian effects are considered, it may be less complicated by adding an unconstrained stochastic process directly to [1.31] – stochastic process adding to [1.28] has to be constrained so as to preserve the unit vector $\mathbf{p}$.

The rheological predictions of this constitutive equation have also been considered by Hinch and Leal Hinch and Leal (1972). In essence, the viscosity is shear thinning, the first normal stress difference is positive, while the second normal stress difference is negative, but of a smaller magnitude. The precise values depend on the aspect ratio and the strength of the Brownian motion. The limit $R \to \infty$ corresponds to a slender particle (prolate spheroid of a large aspect ratio R), and the rest of the discussion is pertinent to this limit.

In a start-up of a shear flow of shear rate $\dot{\gamma}$ (assumed positive here), given an initial state for $\mathbf{p}_0 = \mathbf{Q}_0/Q_0$ expressed as $\{Q_{10}, Q_{20}, Q_{30}\}$, the solution to [1.31] is:

$$\begin{aligned} Q_1 &= Q_{10}\cos\omega t + RQ_{20}\sin\omega t = \left(Q_{10}^2 + R^2Q_{20}^2\right)^{1/2}\cos\left(\omega t - \vartheta\right) \\ Q_2 &= Q_{20}\cos\omega t + R^{-1}Q_{10}\sin\omega t, = \left(R^{-2}Q_{10}^2 + Q_{20}^2\right)^{1/2}\sin\left(\omega t - \vartheta\right) \\ Q_3 &= Q_{30}, \end{aligned} \qquad [1.32]$$

and the frequency of the oscillation is:

$$\omega = \frac{1}{2}\dot{\gamma}\sqrt{\zeta(2-\zeta)} = \frac{\dot{\gamma}R}{R^2+1}, \quad \vartheta = \tan^{-1}\frac{RQ_{20}}{Q_{10}}, \tag{1.33}$$

where $\zeta = 2/\left(R^2+1\right)$. Thus, the particles tumble along with the flow, with a period of $T = 2\pi/\omega = 2\pi(R^2+1)/\dot{\gamma}R = O\left(R/\dot{\gamma}\right)$, spending most of their time aligned with the flow to within an angle $O\left(R^{-1}\right)$ from the flow-vorticity plane. Then, it quickly flips through the remaining orbit in a fraction $O\left(R^{-1}\right)$ of the period.

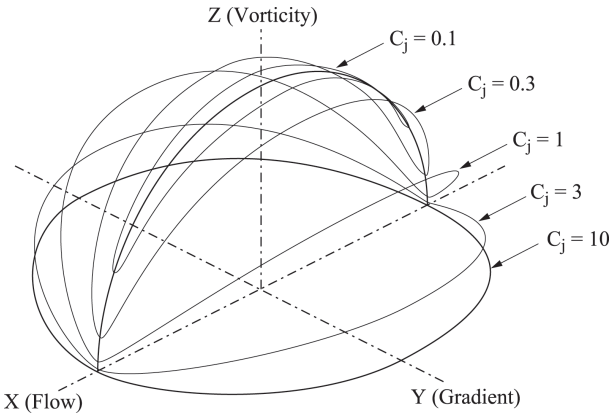

Figure 1.2. *Some Jeffery's orbits at $R = 20$. Each orbit has a unique orbital constant. Orbit of $C_j = 0$ reduces to a point on the vorticity axis; orbit $C_j = \infty$ is located on the flow-gradient plane*

The projection of the orbit of $\mathbf{Q}$ on the flow-gradient plane is an elliptic family:

$$\frac{Q_1^2(t)}{Q_{10}^2 + R^2Q_{20}^2} + \frac{R^2Q_2^2(t)}{Q_{10}^2 + R^2Q_{20}^2} = 1 \tag{1.34}$$

at a distance Q_{30} to the flow-gradient plane. This is usually referred to as Jeffery's orbit. The initial position and the aspect ratio of the particle completely determine the orbit of $\mathbf{Q}$ and, consequently, of $\mathbf{p}$. The orbital constant C_j is defined as:

$$C_j = \frac{\left(Q_{10}^2 + R^2Q_{20}^2\right)^{1/2}}{RQ_{30}} = \frac{\left(Q_1^2 + R^2Q_2^2\right)^{1/2}}{RQ_3} = \frac{\left(p_1^2 + R^2p_2^2\right)^{1/2}}{Rp_3}. \tag{1.35}$$

To avoid singular values, a modified orbital constant $C_b = C_j/(1+C_j)$, $0 < C_b < 1$, is sometimes used.

The suspension viscometric properties are recorded below:

The reduced viscosity:

$$\frac{\langle \sigma_{12} \rangle}{\eta_s \dot{\gamma}} = \mu_r = 1 + \left\langle 2Ap_1^2 p_2^2 + B\left(p_1^2 + p_2^2\right) + C \right\rangle \phi, \qquad [1.36]$$

the reduced first normal stress difference:

$$\frac{N_1}{\eta_s \dot{\gamma}} = 2A \left\langle p_1 p_2 \left(p_1^2 - p_2^2\right) \right\rangle \phi, \qquad [1.37]$$

and the reduced second normal stress difference:

$$\frac{N_2}{\eta_s \dot{\gamma}} = 2 \left\langle p_1 p_2 \left(Ap_2^2 + B\right) \right\rangle \phi. \qquad [1.38]$$

It has been known through simulation that $\langle p_1 p_2 \rangle$ is negative in shear flow, and consequently N_2 would be negative, while N_1 can be either negative or positive. Note also that all the viscometric functions are proportional to the shear rate (strictly speaking, normal stress differences are proportional to the absolute value of the shear rate).

In the start-up of an elongational flow with a (positive) elongational rate $\dot{\gamma}$, the solution for Jeffery's orbit is:

$$\begin{aligned} Q_1 &= Q_{10} \exp\left\{(1-\zeta)\dot{\gamma}t\right\}, \\ Q_2 &= Q_{20} \exp\left\{-\frac{1}{2}(1-\zeta)\dot{\gamma}t\right\}, \\ Q_3 &= Q_{30} \exp\left\{-\frac{1}{2}(1-\zeta)\dot{\gamma}t\right\}, \end{aligned} \qquad [1.39]$$

so that the particle is quickly aligned with the flow in a time scale $O(\dot{\gamma}^{-1})$. The stress can be calculated and, in particular, the reduced elongational viscosity of the suspension is:

$$\frac{N_1}{\eta_s \dot{\gamma}} = \mu_{re} = 3 + (2A + 2B + C)\,\phi \approx \frac{\phi R^2}{\ln 2R - 1.5}. \qquad [1.40]$$

For a dilute suspension of rod-like particle:

$$\mu_{re} \approx 3 + \frac{\phi R^2}{\ln 2R - 1.5}, \qquad [1.41]$$

suggesting an $O\left(R^2\right)$ dependence of the elongational viscosity on the aspect ratio. However, the dilute assumption means that the volume fraction is low enough so that a particle can rotate freely without any hindrance from its nearby neighbors. The distance Δ between any two particles must therefore satisfy $l < \Delta$, where l is the length of a particle of diameter d, so that a volume of l^3 contains only one particle. The volume fraction, therefore, satisfies:

$$\phi \sim \frac{d^2 l}{\Delta^3}, \quad \phi R^2 = \frac{l^3}{\Delta^3} < 1.$$

Thus, the reduced elongational viscosity is only $O(1)$ in the dilute limit, and not $O(R^2)$. Jeffery's solution may be used for a rod-like particle when the aspect ratio R has to be replaced by an effective aspect ratio, $R_e \approx 0.7R$ Cox (1971).

As the concentration increases, we get subsequently into the semi-dilute regime ($1 < \phi R^2 < R$), the concentrated regime ($\phi R > 1$) and the liquid crystalline solution ($\phi R \gg 1$). In the concentrated regime, where the average distance between fibers is less than a fiber diameter, the fibers cannot rotate independently except around their symmetry axes. Any motion of the fiber must necessarily involve a cooperative motion of surrounding fibers. The readers are referred to Doi and Edwards (1988) for more details. Later chapters (Chapters 4–5) deal with the modeling at non-dilute concentrations.

NOTE. As the concentration increases, we get subsequently into the semi-dilute regime ($1 < \phi R^2 < R$), the concentrated regime ($\phi R > 1$) and the liquid crystalline solution ($\phi R \gg 1$). In the concentrated regime, where the average distance between fibers is less than a fiber diameter, the fibers cannot rotate independently except around their symmetry axes. Any motion of the fiber must necessarily involve a cooperative motion of surrounding fibers. The readers are referred to Doi and Edwards (1988) for more details. Later chapters (Chapters 4–5) deal with the modeling at non-dilute concentrations.

THEOREM.– *As the concentration increases, we get subsequently into the semi-dilute regime ($1 < \phi R^2 < R$), the concentrated regime ($\phi R > 1$) and the liquid crystalline solution ($\phi R \gg 1$). In the concentrated regime, where the average distance between fibers is less than a fiber diameter, the fibers cannot rotate independently except around their symmetry axes. Any motion of the fiber must necessarily involve a*

cooperative motion of surrounding fibers. The readers are referred to Doi and Edwards (1988) for more details. Later chapters (Chapters 4–5) deal with the modeling at non-dilute concentrations.

IMPORTANT. As the concentration increases, we get subsequently into the semi-dilute regime ($1 < \phi R^2 < R$), the concentrated regime ($\phi R > 1$) and the liquid crystalline solution ($\phi R \gg 1$). In the concentrated regime, where the average distance between fibers is less than a fiber diameter, the fibers cannot rotate independently except around their symmetry axes. Any motion of the fiber must necessarily involve a cooperative motion of surrounding fibers. The readers are referred to Doi and Edwards (1988) for more details. Later chapters (Chapters 4–5) deal with the modeling at non-dilute concentrations.

As the concentration increases, we get subsequently into the semi-dilute regime ($1 < \phi R^2 < R$), the concentrated regime ($\phi R > 1$) and the liquid crystalline solution ($\phi R \gg 1$). In the concentrated regime, where the average distance between fibers is less than a fiber diameter, the fibers cannot rotate independently except around their symmetry axes. Any motion of the fiber must necessarily involve a cooperative motion of surrounding fibers. The readers are referred to Doi and Edwards (1988) for more details. Later chapters (Chapters 4–5) deal with the modeling at non-dilute concentrations.

As the concentration increases, we get subsequently into the semi-dilute regime ($1 < \phi R^2 < R$), the concentrated regime ($\phi R > 1$) and the liquid crystalline solution ($\phi R \gg 1$). In the concentrated regime, where the average distance between fibers is less than a fiber diameter, the fibers cannot rotate independently except around their symmetry axes. Any motion of the fiber must necessarily involve a cooperative motion of surrounding fibers. The readers are referred to Doi and Edwards (1988) for more details. Later chapters (Chapters 4–5) deal with the modeling at non-dilute concentrations.

As the concentration increases, we get subsequently into the semi-dilute regime ($1 < \phi R^2 < R$), the concentrated regime ($\phi R > 1$) and the liquid crystalline solution ($\phi R \gg 1$). In the concentrated regime, where the average distance between fibers is less than a fiber diameter, the fibers cannot rotate independently except around their symmetry axes. Any motion of the fiber must necessarily involve a cooperative motion of surrounding fibers. The readers are referred to Doi and Edwards (1988) for more details. Later chapters (Chapters 4–5) deal with the modeling at non-dilute concentrations.

As the concentration increases, we get subsequently into the semi-dilute regime ($1 < \phi R^2 < R$), the concentrated regime ($\phi R > 1$) and the liquid crystalline solution ($\phi R \gg 1$). In the concentrated regime, where the average distance between fibers is less than a fiber diameter, the fibers cannot rotate independently except around their symmetry axes. Any motion of the fiber must necessarily involve a cooperative motion of surrounding fibers. The readers are referred to Doi and Edwards (1988) for more details. Later chapters (Chapters 4–5) deal with the modeling at non-dilute concentrations.

As the concentration increases, we get subsequently into the semi-dilute regime ($1 < \phi R^2 < R$), the concentrated regime ($\phi R > 1$) and the liquid crystalline solution ($\phi R \gg 1$). In the concentrated regime, where the average distance between fibers is less than a fiber diameter, the fibers cannot rotate independently except around their symmetry axes. Any motion of the fiber must necessarily involve a cooperative motion of surrounding fibers. The readers are referred to Doi and Edwards (1988) for more details. Later chapters (Chapters 4–5) deal with the modeling at non-dilute concentrations.

Box 1.1. *Caption*

1.6. Bibliography

A.N. Norris, A. C., Sheng, P. (1985), *J. Mech. Phys.*, 33, 525–543.

Batchelor, G. (1970), title, *J. Fluid Mech.*, 44, 545–570.

Cox, R. (1971), *J. Fluid Mech.*, 45, 625–657.

Dai, S.-C., Bertevas, E., Qi, F., Tanner, R. I. (2013), Viscometric functions for noncolloidal sphere suspensions with Newtonian matrices, *Journal of Rheology*, 57(2), 493–510.

Doi, M., Edwards, S. (1988), *The Theory of Polymer Dynamics*, Oxford University Press, Oxford.

Einstein, A. (1956), *Investigations on the Theory of the Brownian Movement*, Ed. R. Fürth, R., New York.

Ericksen, J. (1960), *Kolloid-Z.*, 173, 117–122.

Folgar, F., Tucker, C. (1984), *J. Reinforced Plast. Compos.*, 3, 98–119.

Foss, D., Brady, J. (2000), title, *J. Fluid Mech.*, 407, 167.

Gadala-Maria, F., Acrivos, A. (1980), Shear-induced structure in a concentrated suspension of solid spheres, *Journal of Rheology*, 24(6), 799–814.

Goddard, J., Miller, C. (1967), , 28, 657.

Hand, G. (1961), *Arch Ration Mech Anal*, 7, 81–86.

Happel, J., Brenner, H. (1973), *Low Reynolds Number Hydrodynamics*, Noordhoff International Publishing, Leyden.

Hinch, E., Leal, L. (1972), *J. Fluid Mech.*, 52, 683–712.

Jeffery, G. (1922), *Proc. Roy. Soc. Lond. A*, 102, 161–179.

Kim, S.and Karrila, S. (1991), *Microhydrodynamics: Principles and Selected Applications*, Butterworth and Heinemann, Boston.

Landau, L., Lifshitz, E. (1959), *Fluid Mechanics*, Pergamon Press, New York.

Leal, L., Hinch, E. (1973), *Rheologica Acta*, 12, 127–132.

Lin, Y., Phan-Thien, N., Cheong Khoo, B. (2014), Normal stress differences behavior of polymeric particle suspension in shear flow, *Journal of Rheology*, 58(1), 223–235.

Lyon, M. K., Mead, D. W., Elliott, R. E., Leal, L. G. (2001), Structure formation in moderately concentrated viscoelastic suspensions in simple shear flow, *Journal of Rheology*, 45(4), 881–890.

Mall-Gleissle, S., Gleissle, W., McKinley, G., Buggisch, H. (2002), The normal stress behaviour of suspensions with viscoelastic matrix fluids, *Rheologica Acta*, 41(1-2), 61–76.

Metzner, A. B. (1985), Rheology of suspensions in polymeric liquids, *Journal of Rheology*, 29(6), 739–775.

Mewis, J., Wagner, N. (2012), *Colloidal Suspension Rheology*, Cambridge University Press, New York.

Morris, J. (2009), title, *Rheologica Acta*, 48, 909–923.

Norris, A. (1985), *Mech. Mat.*, 4, 1–16.

Pan, W., Caswell, B., Karniadakis, G. E. (2010), Rheology, Microstructure and Migration in Brownian Colloidal Suspensions, *LANGMUIR*, 26(1), 133–142.

Phan-Thien, N., Fan, X.-J., Khoo, B. (1999), *Rheologica Acta*, 38, 297–304.

Phan-Thien, N., Kim, S. (1994), *Microstructure in Elastic Media Principles and Computational Methods*, Oxford University Press, New York.

Phan-Thien, N., Pham, D. (1997), Differential multiphase models for polydispersed suspensions and particulate solids, *Journal of Non-Newtonian Fluid Mechanics*, 72(2-3), 305 – 318.

Roscoe, R. (1952), *British J. Appl. Phys.*, 3, 267–269.

Tanner, R. I., Qi, F., Housiadas, K. D. (2010), A differential model for the rheological properties of concentrated suspensions with weakly viscoelastic matrices, *Rheologica Acta*, 49(2), 169–176.

Zarraga, I. E., Hill, D. A., Leighton, D. T. (2000), The characterization of the total stress of concentrated suspensions of noncolloidal spheres in newtonian fluids, *Journal of Rheology*, 44(2), 185–220.

Zarraga, I. E., Hill, D. A., Leighton, D. T. (2001), Normal stresses and free surface deformation in concentrated suspensions of noncolloidal spheres in a viscoelastic fluid, *Journal of Rheology*, 45(5), 1065–1084.

Part **1**

Part title

Introduction

As the concentration increases, we get subsequently into the semi-dilute regime ($1 < \phi R^2 < R$), the concentrated regime ($\phi R > 1$) and the liquid crystalline solution ($\phi R \gg 1$). In the concentrated regime, where the average distance between fibers is less than a fiber diameter, the fibers cannot rotate independently except around their symmetry axes. Any motion of the fiber must necessarily involve a cooperative motion of surrounding fibers. The readers are referred to Doi and Edwards (1988) for more details. Later chapters (Chapters 4–5) deal with the modeling at non-dilute concentrations.

Appendix **A**

Appendix title

As the concentration increases, we get subsequently into the semi-dilute regime ($1 < \phi R^2 < R$), the concentrated regime ($\phi R > 1$) and the liquid crystalline solution ($\phi R \gg 1$). In the concentrated regime, where the average distance between fibers is less than a fiber diameter, the fibers cannot rotate independently except around their symmetry axes. Any motion of the fiber must necessarily involve a cooperative motion of surrounding fibers. The readers are referred to Doi and Edwards (1988) for more details. Later chapters (Chapters 4–5) deal with the modeling at non-dilute concentrations.